TECHNISCHE MECHANIK, 32, 2-5, (2012), 518 - 529
submitted: October 28, 2011

Concept of an Agent-stress Model of a Tissue

E. Postek

This paper stands for a concept of coupling between agent modeling and stress analysis valid for a tissue. The stress analysis of evolving tissue is underestimated in previous studies. The experimental observations and numerical simulations of stress development in a single cell and in particular, in a growing tissue are still rare in the literature. We use a tensegrity model for a single cell that serves for stress evaluation in a growing tissue. We propose to couple the mechanical modeling with the agent one using a staggered scheme for two exemplary scenarios. The first example is devoted to scratching of the epithelium, and the second one to the pins and slits. We observe the systems sensitivities with respect to the selected groups of design parameters. The groups of parameters have been associated with clusters of cells. We have found that the sensitivities may be used for comparing the complex structures of the tissue.

1 Introduction

The mechanical environment is important for the behavior of the cells. It influences the cell performance. We stress the following statement: Change the mechanical stresses experienced by cancer cells and they may start to behave more like healthy ones, Ainsworth (2008). The observation of stress development in a single cell and, in particular, in a growing tissue is still rare. The same concerns the numerical simulations. The growing epithelial tissue while treating each cell as an agent is modeled by Sun Tao *et al.* (2007) and Adra et al. (2010). This is done using FLAME (Flexible Large-scale Agent Modelling Environment), Adra et al. (2008). The behaviour of the layer of cells with growing single cells is shown by Postek et al. (2009). We propose a concept of coupling between agent modelling and the stress analysis. The scheme is analogous to the work presented by Park and Felippa (1980) for transient mechanical systems. The two-way coupling is applied to thermomechanical systems by Postek et al (2005).

2 Remark on General Algorithm

The algorithm is based on the well-known idea of staggered solution by Park and Felippa (1980) which was applied to the transient mechanical systems. The scheme was also applied to thermomechanical problems by Lewis et al. (2006) and Postek et al. (2008). The scheme is given in Figure 1. In this case, the T-module is the agent module and the M-module is the mechanical one. The solution from the agent module is transferred to the mechanical module and the feedback from the mechanical module is transferred to the agent module for the next time step.

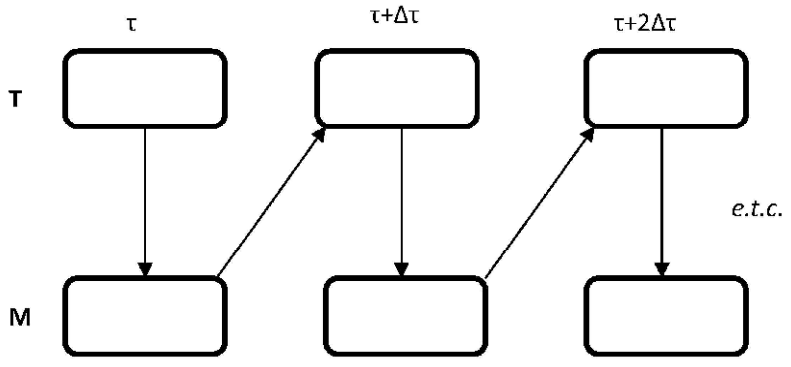

Figure 1. Staggered scheme

3 Characterization of the Agent Model.

A brief characterization of the model is shown in this section. It follows Sun et. al (2007) and the report by Adra et. al (2008). Each cell is treated as an agent. The cells communicate by sending and receiving information while exchanging data on their type and positions. The cells act accordingly to a cell cycle. They divide, differentiate and migrate. Their functions depend on the calcium concentration in the environment. The simple division of stem cells is shown in Figure 2. It can be seen looking at the most left three clusters of the cells. While the cluster becomes big enough the stem cells can differentiate into Transit Amplifying cells. An example of such situation is seen in Figure 1 again in the most right cluster. The TA cell is indicated as a ring.

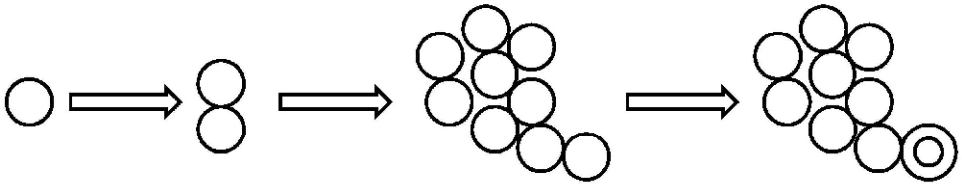

Figure 2. Stem cells differentiate into Transit Amplifying (TA) cells.

When the cluster of stem cells becomes surrounded by TA cells, the TA cells on the edge differentiate into Committed cells, Figure 3 (left). They are shown as black rings. Additionally, the stem cells staying long time in contact can differentiate into Committed cells as well, Figure 3 (right). The TA cells can migrate around the colony depending on the calcium levels. The stem cells stay statically. The Corneocytes are the dead TA and Committed cells.

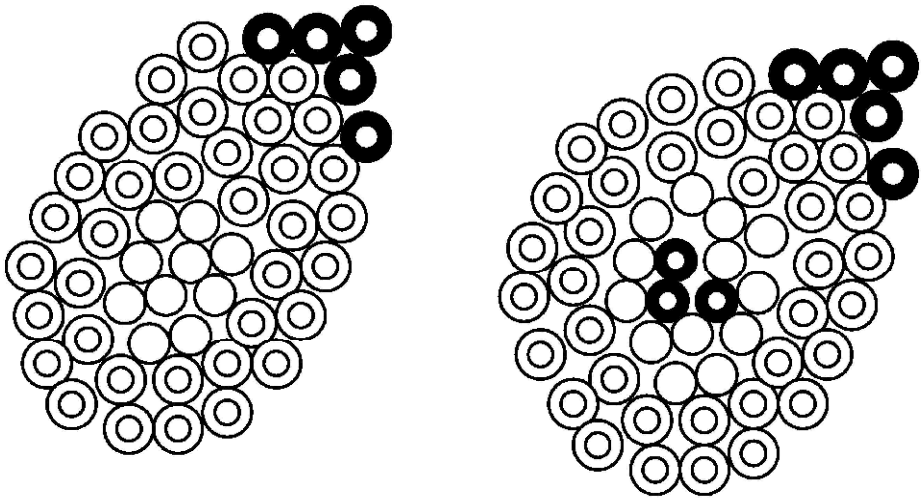

Figure 3. Situations while the Committed Cells appear

4 Example of Colony Formation

To deal with the agent modelling we will use the program FLAME which generates the current state of the tissue. This is demonstrated in Figure 4 (a, b, c). We may see the growth of the cell colony at three time instants. It starts to grow from 6 stem cells (the darkest) and generates 2068 cells at the end of the process. The stem cells produce new stem cells, transit amplifying (TA) cells (fair) and the committed cells (mid-scale of colours). We may see the top layer of committed cells covering a layer of TA cells and several stem cells at the edge of the substrate at the end of the process.

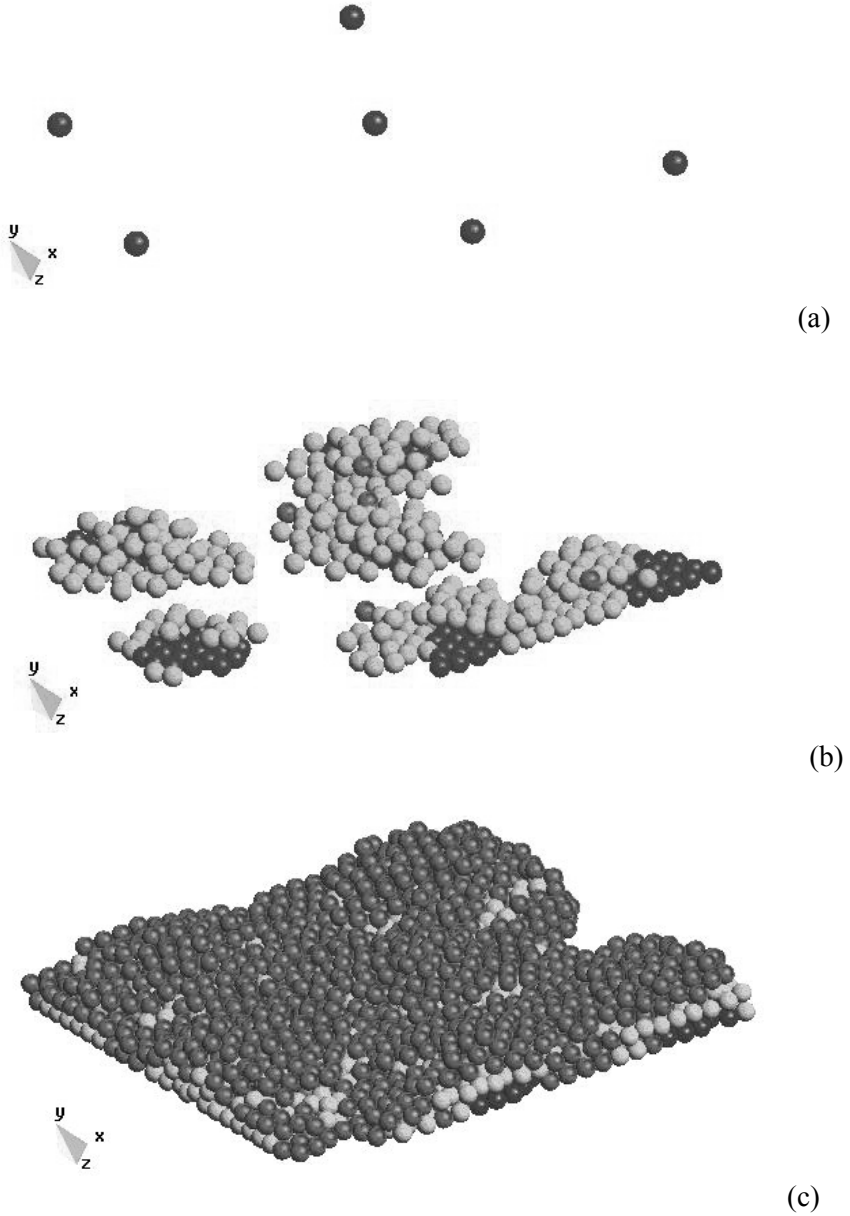

Figure 4. The colony formation; stem cells (a) clusters of cells around stem cells (b) layered structure of tissue (c)

5 Mechanical Module - Design Sensitivity Analysis

We adopt the incremental formulation in the Updated Lagrangian frame, Kleiber *et. al* (1997). The influence of initial stress is exposed via including of the geometrical stiffness matrix.

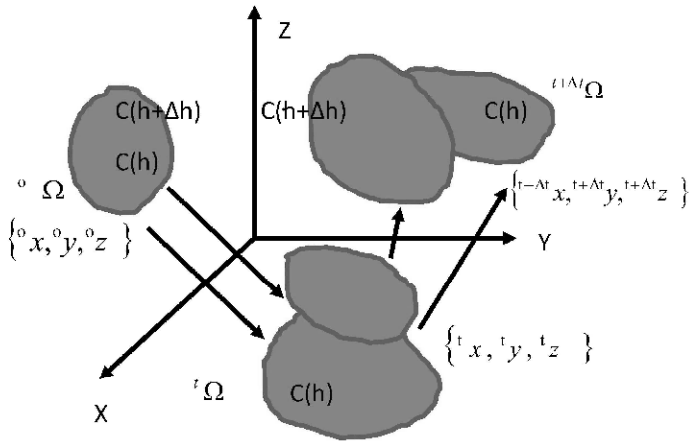

Figure 5. Configurations of the considered body motion

The general idea of the direct differentiation method is shown in Figure 5. There are given the initial, intermediate, and the predicted configurations. The design parameters of the structure are perturbated at the beginning of its motion, and the path of the motion of the perturbed structure differs from the ideal one.
The performance functional valid on the body Ω and its boundary $\partial\Omega_\sigma$ depending on displacements **q**, stresses **S** and design parameter h is of the form

$$ {}^{t+\Delta t}_{t}\Phi = \int_{\Omega^t} {}^{t+\Delta t}_{t}G(\mathbf{S},\mathbf{q},h)d\Omega^t + \int_{\partial\Omega^t_\sigma} {}^{t+\Delta t}_{t}g(\mathbf{q},h)d\left(\partial\Omega^t_\sigma\right) \tag{1} $$

Our goal is to find the derivative of the functional with respect to the design variable h at time $t+\Delta t$. The total potential energy of the nonlinear viscous-elastic system is of the form

$$ \Pi = \int_{\Omega^o} \frac{1}{2} {}^{t+\Delta t}_{o}\mathbf{S} \cdot {}^{t+\Delta t}_{o}\mathbf{E}\, d\Omega^o - \int_{\Omega^o} {}^{t+\Delta t}\mathbf{f}\, {}^{t+\Delta t}\mathbf{u}\, d\Omega^o - \int_{\Omega^t_\sigma} {}^{t+\Delta t}\mathbf{t}\, {}^{t+\Delta t}\mathbf{u} d\left(\partial\Omega^t_\sigma\right) \tag{2} $$

where **S** and **E** are the 2nd Piola-Kirchhof stress tensor and Green-Lagrange strain tensor, **f**, **t** and **u**={u,v,w} are body forces, boundary tractions, and displacements, respectively. All of the values are determined at time t+ Δt in the initial configuration o. In the spirit of the Updated Lagrangian approach we need to transform the equation to the configuration t. Taking the variation of the equation (1) we get the virtual work equation of the form

$$ \delta\Pi = \int_{\Omega^o} {}^{t+\Delta t}_{o}\mathbf{S} \cdot \delta\, {}^{t+\Delta t}_{o}\mathbf{E}\, d\Omega^o - \int_{\Omega^o} {}^{t+\Delta t}\mathbf{f}\, \delta\, {}^{t+\Delta t}\mathbf{u}\, d\Omega^o - \int_{\partial\Omega^o_\sigma} {}^{t+\Delta t}\mathbf{t}\, \delta\, {}^{t+\Delta t}\mathbf{u}\, d\left(\partial\Omega^o_\sigma\right) \tag{3} $$

Exploiting the following relations, e.g. , Malvern (1989)

$$ {}^{t+\Delta t}_{0}\mathbf{S} = \frac{\rho}{\rho_0} {}^{t+\Delta t}_{t}\mathbf{S}, \quad {}^{t+\Delta t}_{0}\mathbf{E} = \frac{\rho}{\rho_0} {}^{t+\Delta t}_{t}\mathbf{E}, \quad \rho d\Omega^t = \rho_0 d\Omega^0 \tag{4} $$

we transform the virtual work equation (2), from the reference configuration at time 0 to the reference configuration at time t. The resulting equation is

$$ \int_{\Omega^t} {}^{t+\Delta t}_{t}\mathbf{S} \cdot \delta\, {}^{t+\Delta t}_{t}\mathbf{E} d\Omega^t = \int_{\Omega^t} {}^{t+\Delta t}\mathbf{f}\, \delta\, {}^{t+\Delta t}\mathbf{u} d\Omega^t + \int_{\partial\Omega^t_\sigma} {}^{t+\Delta t}\mathbf{t}\, \delta\, {}^{t+\Delta t}\mathbf{u} d\left(\partial\Omega^t_\sigma\right) \tag{5} $$

The goal becomes now to obtain the final incremental form of the virtual work equation before discretization. Firstly, the incremental decomposition is employed

$$
\begin{aligned}
&{}^{t+\Delta t}_{t}\mathbf{E} = {}^{t}_{t}\mathbf{E} + \Delta\mathbf{E}, \quad {}^{t+\Delta t}_{t}\mathbf{S} = {}^{t}_{t}\mathbf{S} + \Delta\mathbf{S}, \quad {}^{t+\Delta t}\mathbf{u} = {}^{t}\mathbf{u} + \Delta\mathbf{u}, \\
&{}^{t+\Delta t}\mathbf{f} = {}^{t}\mathbf{f} + \Delta\mathbf{f}, \quad {}^{t+\Delta t}\mathbf{t} = {}^{t}\mathbf{t} + \Delta\mathbf{t}
\end{aligned} \tag{6}
$$

Secondly, the following relations for stress increments holds

$$
\Delta\mathbf{E} = \Delta\mathbf{e} + \Delta\boldsymbol{\eta}, \quad \Delta\mathbf{e} = \overline{\mathbf{A}}\Delta\mathbf{u}, \quad \Delta\boldsymbol{\eta} = \frac{1}{2}\overline{\overline{\mathbf{A}}}(\Delta\mathbf{u}')\Delta\mathbf{u}' \tag{7}
$$

where $\underline{\Delta\mathbf{u}}'$ is the vector of the increment of the displacement derivatives with respect to Cartesian coordinates, and $\overline{\mathbf{A}}$, $\overline{\overline{\mathbf{A}}}$ are the linear and nonlinear operators as follows

$$
\overline{\mathbf{A}} = \begin{bmatrix}
\partial/\partial x & 0 & 0 & \partial/\partial y & \partial/\partial z & 0 \\
0 & \partial/\partial y & 0 & \partial/\partial x & 0 & \partial/\partial z \\
0 & 0 & \partial/\partial z & 0 & \partial/\partial x & \partial/\partial y
\end{bmatrix}^T \tag{8}
$$

$$
\overline{\overline{\mathbf{A}}} = \begin{bmatrix}
\Delta u'_x & 0 & 0 & \Delta v'_x & 0 & 0 & \Delta w'_x & 0 & 0 \\
0 & \Delta u'_y & 0 & 0 & \Delta v'_y & 0 & 0 & \Delta w'_y & 0 \\
0 & 0 & \Delta u'_z & 0 & 0 & \Delta v'_z & 0 & 0 & \Delta w'_z \\
\Delta u'_y & \Delta u'_x & 0 & \Delta v'_y & \Delta v'_x & 0 & \Delta w'_y & \Delta w'_x & 0 \\
0 & \Delta u'_z & \Delta u'_y & 0 & \Delta v'_z & \Delta v'_y & 0 & \Delta w'_z & \Delta w'_y \\
\Delta u'_z & 0 & \Delta u'_x & \Delta v'_z & 0 & \Delta v'_x & \Delta w'_z & 0 & \Delta w'_x
\end{bmatrix} \tag{9}
$$

When substituting the relations (6, 7, 8) into the virtual work equation (5) we obtain

$$
\int_{\Omega^t}\left({}^{t}_{t}\boldsymbol{\tau}\cdot\delta\boldsymbol{\eta} + \Delta\mathbf{S}\cdot\delta\Delta\mathbf{e}\right)d\Omega^t = \int_{\Omega^t}{}^{t+\Delta t}\mathbf{f}\,\delta^{\,t+\Delta t}\mathbf{u}\,d\Omega^t \quad + \int_{\partial\Omega^t_\sigma}{}^{t+\Delta t}\mathbf{t}\,\delta^{\,t+\Delta t}\mathbf{u}\,d(\partial\Omega^t_\sigma) - \int_{\Omega^t}{}^{t}_{t}\boldsymbol{\tau}\cdot\delta\Delta\mathbf{e}\,d\Omega^t \tag{10}
$$

The equation above should be solved iteratively. However, we assume that the equation is fulfilled precisely at time t and all iterations are already done. We obtain the following form of the incremental virtual work equation

$$
\int_{\Omega^t}({}^{t}_{t}\boldsymbol{\tau}\cdot\delta\boldsymbol{\eta} + \Delta\mathbf{S}\cdot\delta\Delta\mathbf{e})\,d\Omega^t = \int_{\Omega^t}\Delta\mathbf{f}\,\delta\Delta\mathbf{u}\,d\Omega^t + \int_{\partial\Omega^t_\sigma}\Delta\mathbf{t}\delta\Delta\mathbf{u}\,d(\partial\Omega^t_\sigma) \tag{11}
$$

We employ the finite element approximation

$$
\Delta\mathbf{u} = \mathbf{N}\Delta\mathbf{q}, \quad \Delta\mathbf{u}' = \mathbf{B}'_L\Delta\mathbf{q} \tag{12}
$$

where $\mathbf{N}$ is the set of shape functions and $\Delta\mathbf{q}$ is the increment of nodal displacements. Let's consider the following set of equalities

$$
{}^{t}_{t}\boldsymbol{\tau}^{\mathrm{T}}\delta\boldsymbol{\eta} = {}^{t}_{t}\boldsymbol{\tau}\,\delta(\overline{\overline{\mathbf{A}}})\Delta\mathbf{u}' = \delta(\Delta\mathbf{u}')^{\mathrm{T}}\,{}^{t}_{t}\overline{\boldsymbol{\tau}}\,\Delta\mathbf{u}' = \delta(\Delta\mathbf{q})^{\mathrm{T}}\,\mathbf{B}'_L \tag{13}
$$

where ${}^{t}_{t}\overline{\boldsymbol{\tau}}$ is the Cauchy matrix and $\mathbf{B}'_L$ and $\mathbf{B}_L$ are the nonlinear and linear operators.

$$
\overline{\boldsymbol{\tau}} = \begin{bmatrix}
{}^{t}_{t}\underline{\boldsymbol{\tau}} & & \\
& {}^{t}_{t}\underline{\boldsymbol{\tau}} & \\
& & {}^{t}_{t}\underline{\boldsymbol{\tau}}
\end{bmatrix} \qquad
{}^{t}_{t}\underline{\boldsymbol{\tau}} = \begin{bmatrix}
{}^{t}_{t}\sigma_{xx} & {}^{t}_{t}\tau_{xy} & {}^{t}_{t}\tau_{xz} \\
& {}^{t}_{t}\sigma_{yy} & {}^{t}_{t}\tau_{yz} \\
& & {}^{t}_{t}\sigma_{zz}
\end{bmatrix} \tag{14}
$$

We obtain the following discretized form of the virtual work equation

$$
\left(\left(\int_{\Omega^t}\mathbf{B}'^{T}_{L}\,{}^{t}_{t}\overline{\boldsymbol{\tau}}\,\mathbf{B}'_L\,d\Omega^t\right)\Delta\mathbf{q} + \int_{\Omega^t}\mathbf{B}^T_L\Delta\mathbf{S}\,d\Omega^t\right) = \int_{\Omega^t}\mathbf{N}^T\Delta\mathbf{f}\,d\Omega^t + \int_{\partial\Omega^t_\sigma}\mathbf{N}^T\Delta\mathbf{t}\,d\left(\partial\Omega^t_\sigma\right) \tag{15}
$$

The stress increment depends on the total stress at time t, strain increment and the design variable. Therefore, the definition of the constitutive tangent is as follows

$$\Delta\mathbf{S} = \Delta\mathbf{S}({}_t^t\mathbf{S}, \Delta\mathbf{e}, h)\ , \quad \frac{\partial\Delta\mathbf{S}}{\partial\Delta\mathbf{e}} = \mathbf{C}^{con}\left({}_t^t\mathbf{S}, \Delta\mathbf{e}, h\right) \tag{16}$$

By differentiating the stress increment we obtain

$$\frac{d\Delta\mathbf{S}}{dh} = \frac{\partial\Delta\mathbf{S}}{\partial\Delta\mathbf{e}}\frac{d\Delta\mathbf{e}}{dh} + \frac{\partial\Delta\mathbf{S}}{\partial\mathbf{S}}\frac{d\mathbf{S}}{dh} + \frac{\partial\Delta\mathbf{S}}{\partial h} \tag{17}$$

Employing the definition of the constitutive tensor and the finite element discretization we obtain the form of the stress increment derivative

$$\frac{d\Delta\mathbf{S}}{dh} = \mathbf{C}^{con}\mathbf{B}_L\frac{d\Delta\mathbf{q}}{dh} + \frac{d\Delta\mathbf{S}}{dh}|_{\Delta\mathbf{q}(h)=const} \tag{18}$$

Substituting the stress derivative increment into the equation (15) the equation for the displacement design derivatives is obtained

$$\left(\int_{\Omega^t}\mathbf{B}_L^T\mathbf{C}^{con}\mathbf{B}_L + \int_{\Omega^t}\mathbf{B}_L^{'T}{}_t^t\overline{\boldsymbol{\tau}}\mathbf{B}_L^{'}\right)\frac{d\Delta\mathbf{q}}{dh} = \frac{d\Delta\mathbf{Q}}{dh} - \left[\int_{\Omega^t}\mathbf{B}_L^T\frac{d\Delta\mathbf{S}}{dh}d\Omega^t\,|_{\Delta\mathbf{q}(h)=const} + \int_{\Omega^t}\mathbf{B}_L^{'T}\frac{d_t^t\overline{\boldsymbol{\tau}}}{dh}\mathbf{B}_L^{'}d\Omega^t\Delta\mathbf{q}\right] \tag{19}$$

In short, the design sensitivity equation takes the form

$$\left(\int_{\Omega^t}\mathbf{B}_L^{'T}{}_t^t\overline{\boldsymbol{\tau}}\mathbf{B}_L^{'}d\Omega^t\right)\frac{d\Delta\mathbf{q}}{dh} + \int_{\Omega^t}\mathbf{B}_L^T\mathbf{S}\,d\Omega^t = \frac{d\Delta\mathbf{Q}}{dh} - \frac{d\Delta\mathbf{F}}{dh}|_{\Delta\varepsilon=const} \tag{20}$$

On the right hand side of the equation (21) we have the derivative of the loading increment with respect to the design parameter and the derivative of the internal force increment with respect to the design parameter. To complete the algorithm we need to make two steps. Firstly, accumulate the displacement and the stress design derivative

$$\frac{d\,{}_t^{t+\Delta t}\mathbf{q}}{dh} = \frac{d_t^t\mathbf{q}}{dh} + \frac{d\Delta\mathbf{q}}{dh} \qquad\qquad \frac{d\,{}_t^{t+\Delta t}\mathbf{S}}{dh} = \frac{d_t^t\mathbf{S}}{dh} + \frac{d\Delta\mathbf{S}}{dh} \tag{21}$$

and secondly, calculate the derivative of the performance functional.
The constitutive model is visco-elastic such as the stress increment depends on total stress $\mathbf{S}$, the shear modulus (G), the bulk modulus (K), and the strain increment $\Delta\mathbf{E}$ as follows

$$\Delta\mathbf{S} = \mathbf{C}^{con}(\mathbf{S},\mathbf{G},\mathbf{K})\Delta\mathbf{E}\ , \quad G(t) = G_o + \sum_{i=1}^{n}G_i\exp\left(\frac{t}{\lambda_i}\right) \tag{22}$$

where t is the time and λ_i are the relaxation times of the particular parallel dampers. The equations (22) describe a generalized Maxwell model.

6 Coupling Scheme

The concept of the coupling scheme follows the Figure 1 and is refined considering the functions of the agent and mechanical modules, Figure 6. The agents follow the rules about the differentiation, division and death depicted in the Section 3 and illustrated in Figure 2 and in Figure 3. We need to transfer the data about the actual state (in fact the kind) and position of the cells to the mechanical module. However, before we go into the FEM solver we need to update the geometry, discretization and material data of the model. The latter is due to the differentiation of the cells. Having the update we can solve the model for displacement, stresses and sensitivities. It is possible

to transfer the resulting variables (displacements, stresses, sensitivities) into the agents and deal with the effects of the mentioned fields on the cell cycle.

For Each time step (T-module actions)
For each agent
Read state and position of neighbouring agents
Update state and position as determined by internal rules and external signals
Write new state and position of the agents
End
Update the mechanical model (its geometry)
Transfer data about the state and position to the mechanical module
Assign the appropriate material data to the cells
The tasks of the mechanical module (M-module actions)
Evaluate the state of displacements, strain and stress in the tissue including the cytoskeleton and membranes and the contact forces (mechanotransduction)
Calculate the sensitivities
Feedback to the agents – correct their positions
End

Figure 6. Refined coupling scheme

7 Numerical Aspects

The parallel version of the program includes the solver MUltifrontal Massively Parallel Solver, MUMPS, Amestoy *et. al* (2001) and (2006). We use the Newton-Raphson technique for solving the equation of equilibrium (15). The sensitivity algorithm creates additional right hand sides in the equation (20), for example Kleiber et. al (1994). We need to solve as many right hand sides as the number of design variables. The design sensitivity equation is solved using the triangularized form of the last stiffness obtained in the last iteration loop.

8 Generic Cell

The elementary cell consists of nucleus, actins, microtubules, membrane and collagen. We will deal with the mechanical model of the cytoskeleton. The cytoskeleton consists of actins and microtubules. The actins act as tendons and the microtubules act as compressed struts. They build the tensegrity structure of the cell, Stamenovic (2005). The observed behaviour of the elementary cells is viscoelastic. They are pre-stressed and keep approximately their volume when deformed and they stiffen when undergoing tension.

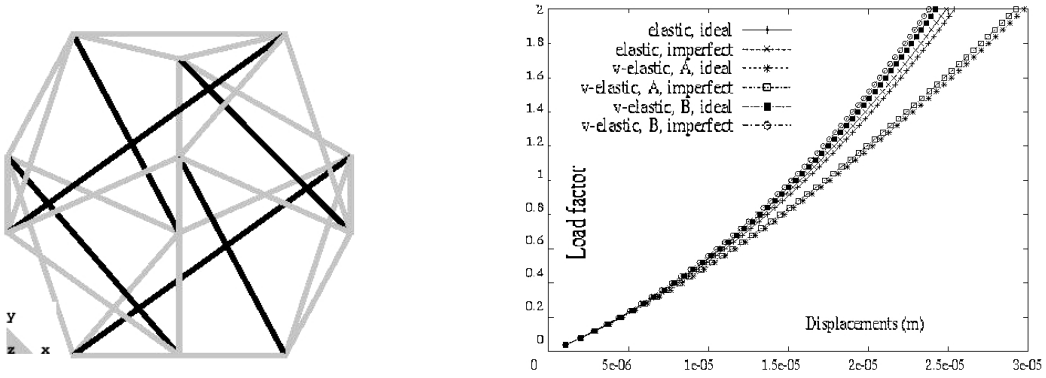

Figure 7. Elementary icosahedron (left) and load-displacement path

These conditions are fulfilled by the elementary icosahedron based tensegrity structure, Figure 7. We deal with the elementary cell model with equivalent actins and microtubules. We adopted the following data, height of the cell 64 μm, cross-sectional areas of the tendons (filaments) $10nm^2$, cross-sectional areas of the struts (microtubules) 190 nm^2, Young's moduli of the tendons 2.6GPa and the struts 1.2GPa, initial prestressing forces 20 nN, maximum loading 0.1N, relaxation time 1.0 sec, G_i/G_o ratio 0.91 (case A) and 0.1 (case B). We may note a certain effect of the imperfect position of the nodes and higher stiffening effect for higher G_i/G_o ratios (case A).

9 Examples of Tissue Behaviour

9.1 Scratch Appearance

We consider a pattern of matrix of cells forming a single layer tissue. We are assuming the same data for each single cell as in the Section 8. The layer of cells can slide and is fixed on its right side preventing rigid body motions, (see Figure 8). It is loaded with the concentrated forces on the left side, each concentrated force is 100.0d-04N. We assume that the tissue is scratched after 0.1 sec of the loading process. We observe the sensitivity fields of the displacements with respect to the design variables such as three cells in which all microtubules can change simultaneously their lengths. The cluster of cells is formed by arbitralily choosen cells but placed in certain distance between each of them. They can qualitatively catch the effect of the simultaneous growth of the cells in the cluster. Such a situation may happen in a real tissue quite often. Obviously, several cells in different places can grow simultaneously. The three cells are a kind of markers.
The displacement sensitivity field is shown in Figure 9.

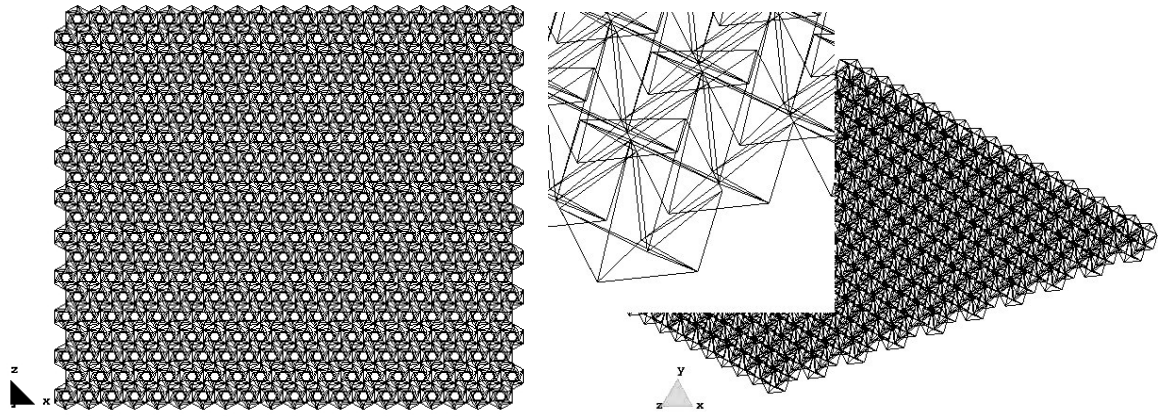

Figure 8. The considered pattern of cells in the single cell layer of the tissue – top view (left), detail of the corner (right)

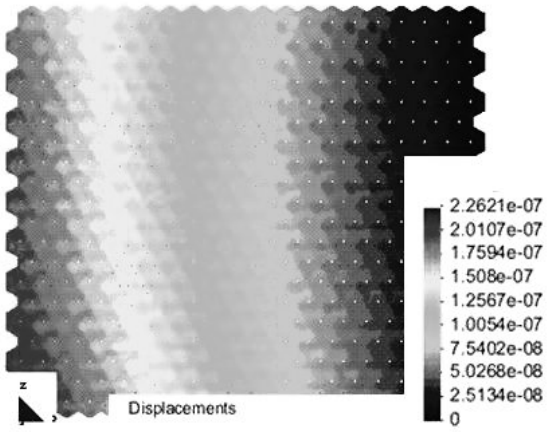

Figure 9. Displacement field in the tissue before the scratch has started

We may note that the most sensitive places in the layer are in the neighbourhood of the cells which can undergo a perturbation. The sensitivities of the system are shown at the beginning of the scratch appearance, Figure 10 (left) and at the end of its development, Figure 10 (right).
We observe that at the beginning of the scratch appearance the most sensitive places are again in the neighbourhood of the choosen cells. However, the picture becomes different at the end of the process. The DSA gradients are becoming regularly distributed on left side of the scratch. It means that the choosen cells have stopped to be the most important. The perturbation of the design parameters in the choosen cells makes similar effects in the entire structure on left side and the gradients are of range higher. This means that the tissue approaches its destruction.

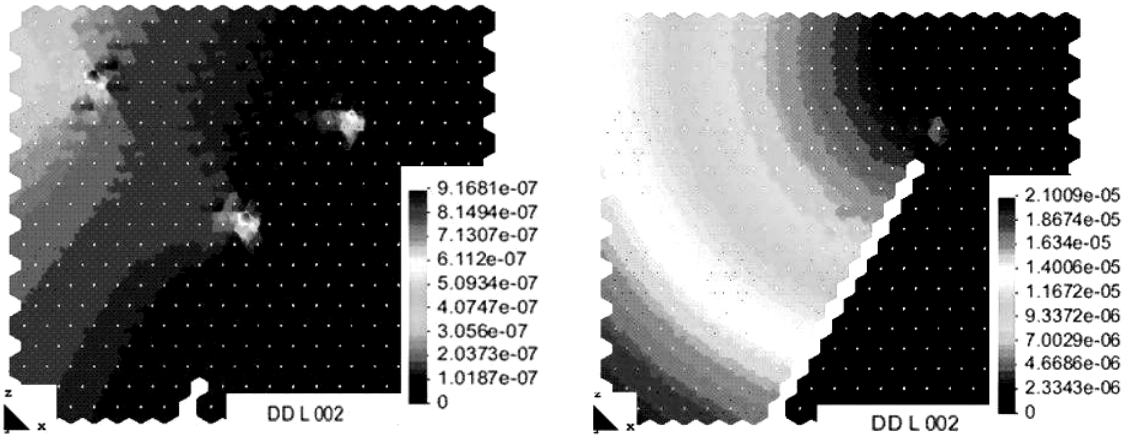

Figure 10. Design sensitivity field at the beginning of the process (left) and at the end of the process (right)

9.2 Holes and Slits

We consider a tissue made of 10000 elementary cells. We observe the sensitivities and demonstrate that the model can catch the effect of the stress concentrations.
The boundary conditions and the loading are the same as in the structure presented above. We will consider the pieces of the tissue with a punched hole and a slit and compare its behaviour with the ideal tissue. The displacement field in the ideal tissue is shown in Figure 11 and the fields in the samples with openings are given in Figure 12.

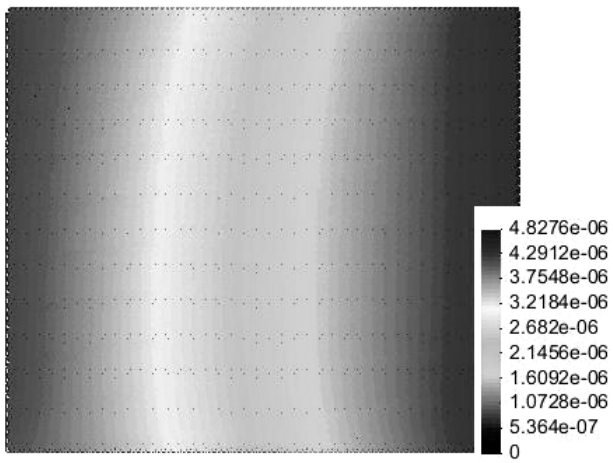

Figure 11. Displacement field in the ideal tissue

We observe that the displacement fields are perturbed around the openings what demonstrates the applicability of the model and the reticular medium to describe the continuous tissue, Figure 12.

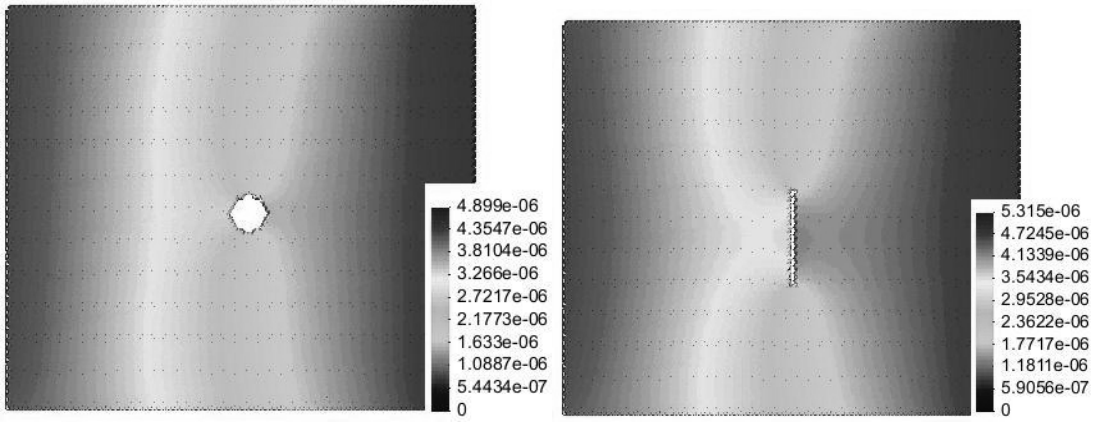

Figure 12. Displacement fields in the tissue with a hole (left) and with a slit (right)

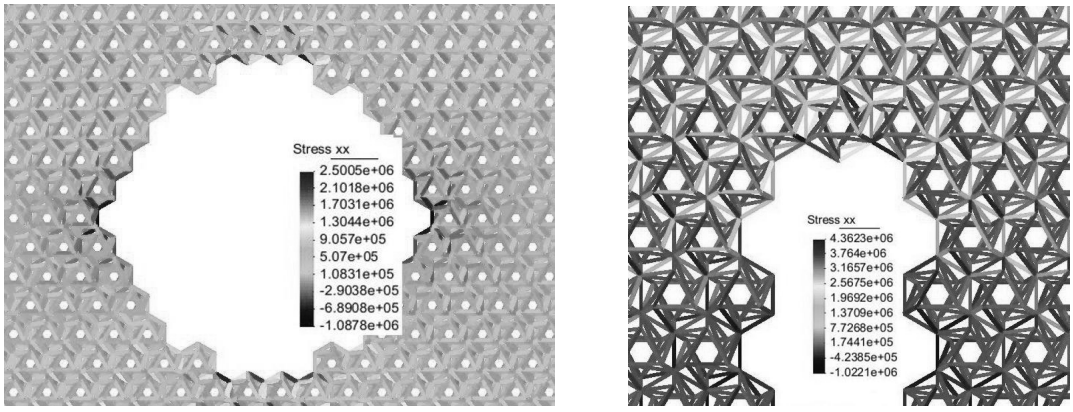

Figure 13. Stress concentrations around the hole (left) and at the tip of the (slit)

The stress concentrations around the hole and around the slit are shown in Figure 13 (left and right). The stresses are significantly higher at the tip of the slit than around the hole.

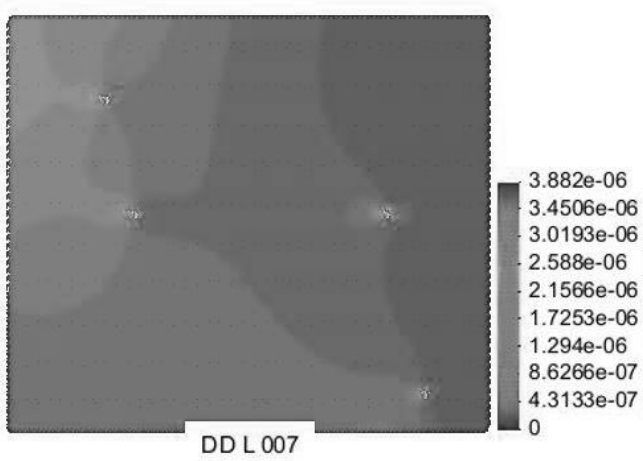

Figure 14. Design sensitivity field in the ideal tissue

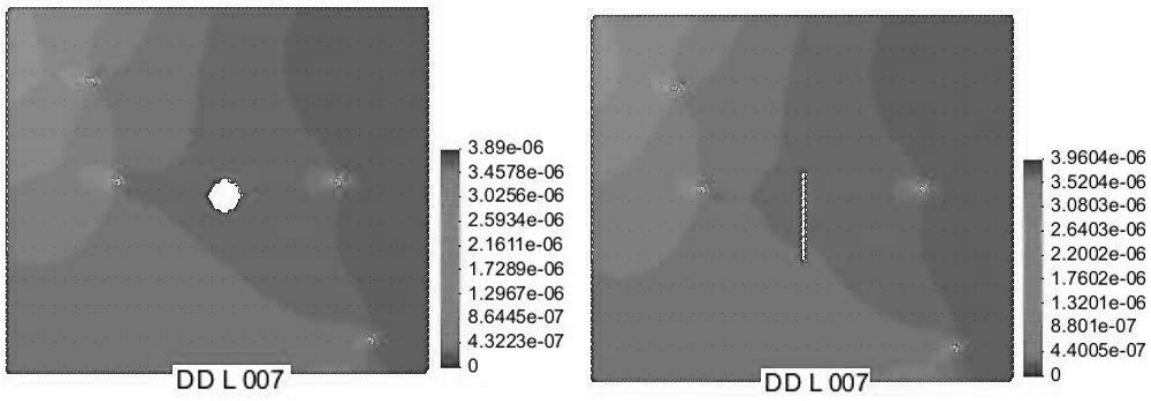

Figure 15. Design sensitivity fields in the tissue with a hole (left) and with a slit (right)

The considered design sensitivity fields are shown in Figures 14 and 15. The design variables are defined as the sum of the lengths of the microtubules in 4 cells. The cells are easily visible since they form hot spots. When comparing the maximum sensitivities we note that the less sensitive to the defined set of the design parameters is the ideal system (Figure 14) and the most sensitive is the system with the slit (Figure 15, right). The system with the hole is moderately sensitive, Figure 15 (left).

10 Final Remarks

It has been presented a concept of coupling scheme between agent models and mechanical models. The mechanical model consists of the implemented design sensitivity algorithm valid for nonlinear path dependent systems. The application of it is the computational systems biology. We have described numerical aspects of the implementation with parallel multifrontal solver and shown numerical examples and possible application of the presented theory.
We can see that the internal structure of the cells interacts with the tissue. The effects can be evaluated using he design sensitivity analysis. The design sensitivity analysis is an appropriate tool to evaluate the effects of the secondary elements of the tissue. The DSA (has this acronym introduced before?) has appeared particularly useful for evaluation of the defects in the tissue and prediction of its behaviour.
The concept of the coupling scheme applied to the tissue is useful for the stress evaluation in the tissue. It naturally arises from the formulation for transient mechanical systems and naturally allows to model the evolving in time structures like living tissue.

11 Acknowledgements

The parallel version of the program was prepared during the research visit in the High Performance Computing Centre (HLRS) and in the Institute of Materials Testing, Materials Science and Strength of Materials (IMWF) at the University of Stuttgart. The work has been performed under the HPC-EUROPA2 project (project number: 228398) with the support of the European Commission - Capacities Area - Research Infrastructures).
The author thanks to the Engineering and Physical Research Council, UK for the support under the grant "The Epitheliome: computational modelling of epithelial tissue", GR/S62321/01

References

Adra, S. F.; Coakley, S.; Kiran, M.; McMinn, P.: An agent-based software platform for modelling systems biology. Epitheliome Project Report, *http://www.flame.ac.uk* (2008).

Adra, S.; Sun, T.; McNeil, S.; Holcombe, M.; Smallwood, R.: Development of a three dimensional multiscale computational model of the human epidermis. *PLoS ONE*, 5, (2010), 1-13.

Ainsworth, C.: Stretching the imagination. *Nature,* 456, (2008), 696-699.

Amestoy P. R.; Duff I.S.; Koster J.; L'Excellent J.-Y.: A fully asynchronous multifrontal solver using distributed dynamic scheduling. *SIAM Journal of Matrix Analysis and Applications,* 23, (2001), 15-41.

Amestoy, P. R.; Guermouche A.; L'Excellent J.Y.; Pralet S.: Hybrid scheduling for the parallel solution of linear systems. *Parallel Computing*, 32, (2006), 136-156.

Felippa, C. A.; Park, K. C.: Staggered transient analysis procedures for coupled mechanical systems: formulation. *Comput. Methods Appl. Mech. Eng*. 24, (1980), 61-111.

Kleiber M.; Hien, T. D.; Postek, E.: Incremental finite element sensitivity analysis for non-linear mechanics applications. *Int. J. for Numer. Meth. in Eng.,* 37, (1994), 3291-3308.

Kleiber M.; Antunez H.; Hien T.D.; Kowalczyk P.: *Parameter Sensitivity in Nonlinear Mechanics: Theory and Finite Elements*. Wiley & Sons, 1997.

Lewis, R. W.; Postek, E. W.; Han, Z. Q.; Gethin D. T.: A finite element model of the squeeze casting processes. *Int. J. of Numer. Meth. for Heat and Fluid Flow*, 16, (2006), 539-572.

Malvern L.E.: *Introduction to the Continuum Mechanics*. Polish Scientific Publishers and Englewood Cliffs, 1989.

Postek, E. W.; Smallwood, R.; Hose, R.: Nodal positions displacement sensitivity of an elementary icosahedral tensegrity structure. In: *Computational Plasticity, Fundamentals and Applications*, E. Onate; D. R. J. Owen, eds., CD Proceedings of the X International Conference on Computational Plasticity, COMPLAS X, Barcelona, 2-4 September, 2009.

Postek, E. W.; Lewis, R. W.; Gethin, D. T.: Finite element modelling of the squeeze casting process. *Int. J. of Numer. Meth. for Heat and Fluid Flow,* 18, (2008), 325-355.

Postek, E. W.; Lewis, R. W.; Gethin, D. T.; Ransing, R. S.: Influence of initial stresses on the cast behaviour during squeeze forming processes. *J. of Mat. Proc. Tech.,* 159, (2005), 338-346.

Sun, T.; McMinn, P.; Coakley S.; Holcombe, M.; Smallwood, R.; MacNeil, S.: An integrated systems biology approach to understanding the rules of keratinocyte colony formation. *J. Roy. Soc. Interface*, 4, (2007), 1077-1092.

Stamenovic, D.: Effects of cytoskeletal prestress on cell rheological behavior. *Acta Biomater.*, 1, (2005), 255-262.

Address: Dr. Eligiusz Postek, Institute of Fundamental Technological Research of the Polish Academy of Sciences, Pawińskiego 5B, 02-106 Warszawa, Poland
email: epostek@ippt.gov.pl, ewpostek@gmail.com